Research Square

Preprints are preliminary reports that have not undergone peer review.
They should not be considered conclusive, used to inform clinical practice,
or referenced by the media as validated information.

Bioinformatics Identification and Validation of Pyroptosis-Related Diagnostic Biomarkers in Diabetic Nephropathy

Xinru Wang
Shandong University of Traditional Chinese Medicine
Zhaoan Guo
ljxiang1110@163.com

Affiliated Hospital of Shandong University of Traditional Chinese Medicine

Article

Keywords: Diabetic nephropathy, Cell pyroptosis, Machine learning, Molecular docking, Human being

Posted Date: March 26th, 2026

DOI: https://doi.org/10.21203/rs.3.rs-8892178/v1

License: This work is licensed under a Creative Commons Attribution 4.0 International License.
Read Full License

Additional Declarations: No competing interests reported.

First author : Xinru Wang First Clinical Medical College, Shandong University of Traditional Chinese Medicine, Jinan 250014, China; dpwangxinru@163.com
Corresponding author : Zhaoan Guo Nephrology Department, Shandong University of Traditional Chinese Medicine Affiliated Hospital, Jinan 250014, China; ljxiang1110@163.com
Funding Declaration: Supported by Shandong Natural Science Foundation Project (No. ZR2022LZY005)

Bioinformatics Identification and Validation of Pyroptosis-Related Diagnostic Biomarkers in Diabetic Nephropathy

Xinru Wang[1],Zhaoan Guo[2▲]

（1 First Clinical Medical College, Shandong University of Traditional Chinese Medicine, Jinan 250014, China; 2 Corresponding author, Nephrology Department, Affiliated Hospital of Shandong University of Traditional Chinese Medicine, Jinan 250014, China）

Background: Diabetic nephropathy (DN) is a common and serious issue in nephrology. This disease often develops without clear early symptoms. Its causes are complex and multiple. Good markers for early diagnosis are still lacking. Pyroptosis is a form of programmed cell death. It triggers strong inflammatory responses. Emerging evidences indicate that pyroptosis may be involved in the development and progression of DN. **Methods:** In this study, we found genes that are shared by DN and pyroptosis. We then studied key genes in more detail and tested them by using weighted gene co-expression network analysis, machine learning methods, single-cell RNA sequencing, and molecular docking to check their predictive value and reliability. **Results:** We identified two key genes, *MYH9* and *CDC20*. Both genes were highly expressed in podocytes. Functional analysis showed that *MYH9* is mainly related to the immune infiltration of naive B cells and resting mast cells. *CDC20* is related to the immune infiltration of resting mast cells and naive CD4 T cells. Molecular docking and competing endogenous RNA (ceRNA) analysis also supported the diagnostic and

[1] First author : Xinru Wang First Clinical Medical College, Shandong University of Traditional Chinese Medicine, Jinan 250014, China; dpwangxinru@163.com
[2] Corresponding author : Zhaoan Guo Nephrology Department, Shandong University of Traditional Chinese Medicine Affiliated Hospital, Jinan 250014, China; ljxiang1110@163.com
▲ Supported by Shandong Natural Science Foundation Project (No. ZR2022LZY005)

predictive value of *MYH9* and *CDC20* in DN. **Conclusion**: *MYH9* and *CDC20* serve as potential predictive biomarkers elucidating the role of pyroptosis in DN pathogenesis, and may offer promising avenues for early diagnosis and intervention in DN.

Key words: Diabetic nephropathy; Cell pyroptosis; Machine learning; Molecular docking; Human being;

Diabetic nephropathy (DN) is a serious complication of diabetes and a key cause of end-stage renal disease (ESRD). Globally, approximately 30% to 50% of ESRD cased by DN[1]. Currently, there are no simple and effective early diagnostic markers for DN, which leads to many diabetic patients failing to detect the concurrent DN in a timely manner during the progression of the disease. This delaying treatment allows the disease to advance to the end-stage ESRD stage, severely impacting not only the patients, but also posing a significant challenge to socioeconomic development and healthcare resource allocation[2]. The mechanism of DN is complex and involves multiple factors such as impaired glucose metabolism, persistent inflammatory stimulation, oxidative stress, and renal fibrosis[3]. Although numerous measures exist to slow the progression of DN, their effectiveness remains limited. Therefore, it is particularly important to deeply explore the molecular mechanism of DN and seek new treatment and diagnostic strategies.

In patients with DN, elevated levels of adhesion molecules and chemokines and infiltration of immune cells are often observed, which highlights the core role of inflammation in DN. Further exploration of the inflammatory mechanism behind DN will help us find new targets[4]. Pyroptosis is a cell death pathway that expands the inflammatory response and is closely related to the production and progress of DN. The activation of NLRP3 inflammasome is the beginning of pyroptosis, When NLRP3 inflammasome is activated, it will stimulate the formation of cysteinyl aspartate specific proteinase-1 (caspase-1), and then caspase-1 will trigger cell death through dual action. On the one hand, caspase-1 can specifically cleave and expose the N-terminal region of its downstream protein, gasdermin D (gsdmd); On the other hand, caspase-1 can promote the activation of IL-18, IL-1 β and other inflammatory

factor precursors. Finally, the exposed N-terminal region of gsdmd forms holes by dividing the cell membrane, promoting the release of inflammatory factors such as activated IL-18 and IL-1 β outside the membrane, amplifying the inflammatory response and triggering cell death[5,6]. In DN, pyroptosis is not only triggered by inflammatory stimuli, but can also be directly upregulated by the hyperglycemic milieu, which upregulates the level of NLRP3, GSDMD, and caspase-1, thereby sustaining pyroptosis[7,8]. Elevated expression of GSDMD and caspase-11/4, along with excessive activation of pyroptosis, has been observed in DN mouse models, hyperglycemia (HG)-induced human renal tubular epithelial cell (HK-2) models, and in patients with diabetic nephropathy[9,10,11,12]. After pyroptosis, the persistent release of inflammatory mediators not only stimulates renal cells, causing persistent tissue damage, but also promotes the excessive buildup of extracellular matrix and leads to interstitial fibrosis. These effects result in glomerulosclerosis and the progressive fibrosis of kidney tissue. Kidney function is consequently impaired, and the advancement of diabetic nephropathy is accelerated[13,14]. The research also confirmed that in the DN tissue, the activation of NLRP3 is often present[15], knockout of NLRP3 leads to downregulation of pyroptosis-related factors, which significantly alleviates kidney inflammation, glomerulosclerosis, and fibrosis in DN mice. As a result, renal function is preserved and the progression of diabetic nephropathy is delayed.[16,17,18]. Therefore, a comprehensive understanding of the molecular mechanisms by which pyroptosis contributes to the progression of DN may provide a theoretical foundation for identifying novel therapeutic and predictive targets for diabetic nephropathy.

In this study, we first integrated and analyzed the dataset of DN patients from GEO, then intersected it with genes related to pyroptosis. Subsequently, we used weighted gene co-expression network analysis (WGCNA) and three machine learning algorithms to identify pivotal genes associated with pyroptosis and DN. Finally, we verified these hub genes, analyzed the pathway enrichment, cell distribution, immune infiltration, therapeutic drugs, and constructed the Cerna network of hub genes to analyze the essence of DN induced by pyroptosis.

1 Materials and Methods

1.1 Data Sources

In the GEO (Gene Expression Omnibus, https://www.ncbi.nlm.nih.gov/geo/) database, we searched for “diabetes nephropathy” or “Diabetic kidney disease” and identified 2 datasets. GSE30528 (GPL571) was selected as the training set, comprising 9 diabetic nephropathy cases and 13 controls; GSE96804 (GPL17586), comprising 41 diabetic nephropathy cases and 20 controls, served as the validation set. A search for “Pyroptosis” in GeneCards (https://www.genecards.org/) yielded 2,013 pyroptosis-related genes.

1.2 Identification of DEGs

We used the “limma” R package to identify differentially expressed genes (DEGs) in GSE30528, setting the screening criteria as log2 fold change> 0.05 and *p*-value < 0.05[19]. Heatmaps and volcano plots were generated using the ‘Pheatmap’ and “ggplot2” R packages, respectively.

Subsequently, the DEGs were intersected with pyroptosis-related genes to obtain pyroptosis-associated differentially expressed genes (Pyro-DEGs).

1.3 Pyro-DEGs Enrichment Analysis

Functional enrichment analysis of Gene Ontology (GO) and Kyoto Encyclopedia of genes genome (KEGG) was carried out in R using "clusterprofiler", "org.hs.eg.db", "enrichblot" and other packages to evaluate gene related biological processes (BP), molecular functions (MF), cellular components (CC) and gene related signaling pathways[20,21].

1.4 Construction of Weighted Gene Co-expression Network

To pinpoint the key gene modules associated with DN, we used the "WGCNA" package for WGCNA to identify gene coexpression modules by constructing a scale-free topological coexpression network (R^2 >0.90). Then, the module structure was optimized by cutting the dynamic tree and merging the modules with dissimilarity less than 0.25. Subsequently, The Pearson correlation coefficient was

employed to evaluate the relationship between module characteristic genes and clinical traits, and determine the key gene module[22].

Finally, we intersected Pyro-DEGs with key gene modules to identify Pyroptosis-related key co-expressed genes (Pyro-KCoGs).

1.5 Machine Learning Screening of Hub Genes

To screen out hub genes, we used three different machine models, using the "glmnet" package, and selected 10 fold cross validation for least absolute shrinkage and S; selection operator (lasso) regression[23,24], The “randomForest” package performed Random Forest (RF) analysis[25], The optimal number of variables was determined according to the average error rate of differentially expressed genes, and genes with a feature importance score greater than 1 were selected as reference genes; In addition, the "e1071" package was used for support vector machine recursive feature elimination (SVM-RFE) analysis[26], selecting the feature set with the minimum cross validation error rate. Finally, the gene intersection obtained by three machine algorithms is determined as the focal death hub gene.

1.6 Efficacy Evaluation and Validation of Hub Genes

Violin plots and receiver operating characteristic (ROC) curves for both training and validation cohorts were generated to assess the diagnostic performance of hub genes for DN. The diagnostic performance was assessed using the area under the ROC curve (AUC) [27].

1.7 GSEA Analysis

We performed GSEA analysis on the hub genes identified in Section 1.5 to investigate their functional roles[28,29].

1.8 Immune Cell Infiltration

We employed the “Cibersort” package for immune cell infiltration analysis[30], inferring the proportion of each immune cell type in the dataset samples by comparing known immune cell genes with gene expression data from the dataset. Additionally, The relationship between the two hub genes and immune cells was examined using

Pearson correlation tests, considering $|R| \geq 0.5$ and $p < 0.05$ as statistically significant.

1.9 Single-Cell RNA Sequencing

We used the single cell sequencing database of "kidney integrated transcriptome (K.I.T.)"（http://humphreyslab.com/SingleCell/）to explore the distribution of hub genes in cell populations, and we used DN mononuclear RNA sequencing data from the gse131882 dataset, as published by Wilson et al[31], were analyzed.

1.10 Drug Prediction and Molecular Docking

We utilized the DSigDB database within the Enrichr platform (https://maayanlab.cloud/Enrichr/) for drug screening of genes, identifying drug molecules interacting with hub genes (p-value < 0.05 considered significant). The binding affinity between drugs and hub targets was assessed, we performed molecular docking. First, drug components were obtained from the PubChem database (https://pubchem.ncbi.nlm.nih.gov/). Energy was minimized in ChemBio3D (20.0.0.41). Next, we retrieved key genes from the Uniprot database (https://www.uniprot.org/) and obtained their highest-resolution crystal structures. Using PyMOL 3.1.2, we removed ligands and water molecules, then processed the proteins with AutoDock (v1.5.7), including charge assignment, receptor molecule definition, and hydrogenation. Subsequently, molecular docking was performed using AutoDock Vina (v1.1.2) for the drug and target protein. The optimal binding conformation was selected based on the principle of minimum binding free energy. Finally, the complex was visualized using PyMOL to elucidate its binding mode and intermolecular interactions.

1.11 Construction of the ceRNA Network

We predicted miRNAs associated with hub genes from the miRNet (https://www.mirnet.ca/), miRDB (https://mirdb.org/), and starBase (https://rnasysu.com/encori/) databases, and used the starBase database to predict the corresponding lncRNAs for these miRNAs. Finally, a ceRNA regulatory network was generated in Cytoscape 3.9.1.

Results

2.1 Analysis and Identification of DN and Pyroptosis

A total of 549 DEGs were identified from GSE30528, visualized using heatmaps and volcano plots. To further explore the role of pyroptosis in DN, we mined 2,013 pyroptosis-related genes from the Genecards database and intersected them with the DEGs to obtain 68 Pyro-DEGs (Figure 1A-C).

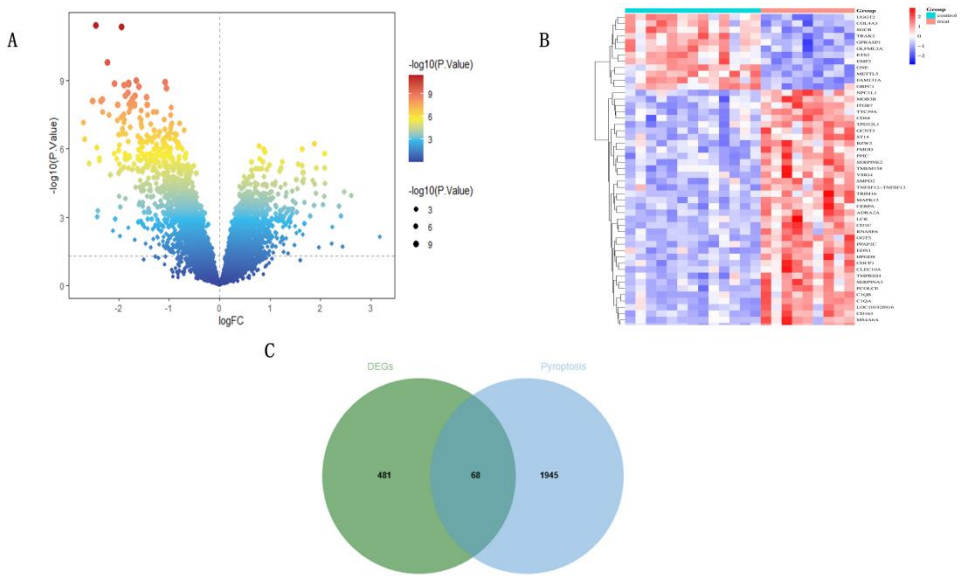


Figure 1 Differential expression analysis of GSE30528.

2.2 GO and KEGG Analysis of Pyro-DEGs

The results showed that in terms of BP, these genes were mainly related to the regulation of leukocyte migration, phagocytosis, tumor necrosis factor and the production of inflammatory response related mediators; As for CC, these genes are significantly correlated with adhesive plaque, cell matrix junction, secretory granule cavity, and cytoplasmic vesicle cavity. Finally, in terms of MF, these genes are mainly related to integrin binding, cytokine receptor binding, actin binding, ribosomal structural components, etc. (Figure 2A and B). In addition, KEGG pathway analysis revealed that these intersection genes are mainly enriched in the immune inflammatory response (e.g Coronavirus disease - COVID-19, Shigellosis, Influenza A）, Cell adhesion and signal transduction (such as focal adhesion, integrity signaling),

hypoxia stress (HIF-1 signaling pathway), and programmed cell death (such as necroptosis, nod like receptor signaling pathway) (Figure 2C and D). Therefore, observations from this study support Pyro-DEGs may play a role in the promotion of DN by pyroptosis through the differential expression of the above signaling pathways.

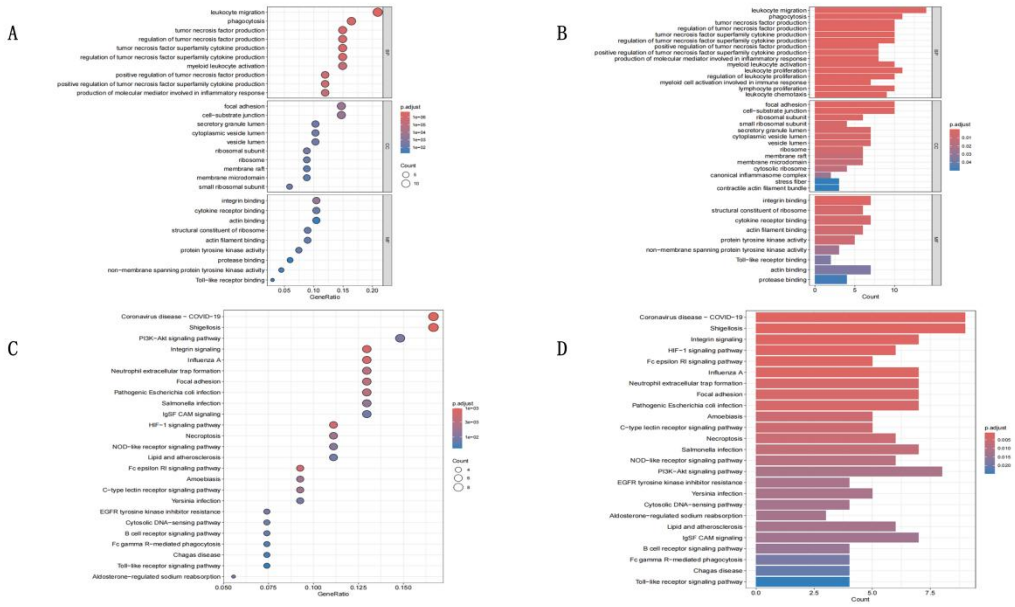


Figure 2 Functional enrichment analysis of pyro DEGs

2.3 Identification of Key Gene Modules

We performed WGCNA on the gene expression data of DN and normal samples. First, the samples are stratified and clustered to remove the abnormal samples (Figure 3A); then, by analyzing the network topology, the soft threshold is determined to be power=11 (R^2=0.85) to build an approximate scale-free network (Figure 3B); The genes are classified by hierarchical clustering and dynamic tree cutting, and highly similar modules are merged (Figure 3C); Finally, WGCNA analyzed a total of 14 modules, and meturquoise had the strongest positive and negative correlation with the clinical phenotype of DN (r=± 0.92), so the turquoise module was regarded as a key gene module (Figure 3D).

We identified overlapping DEGs, pyroptosis genes, and key gene modules from WGCNA, resulting in 12 shared genes (Figure 3E).

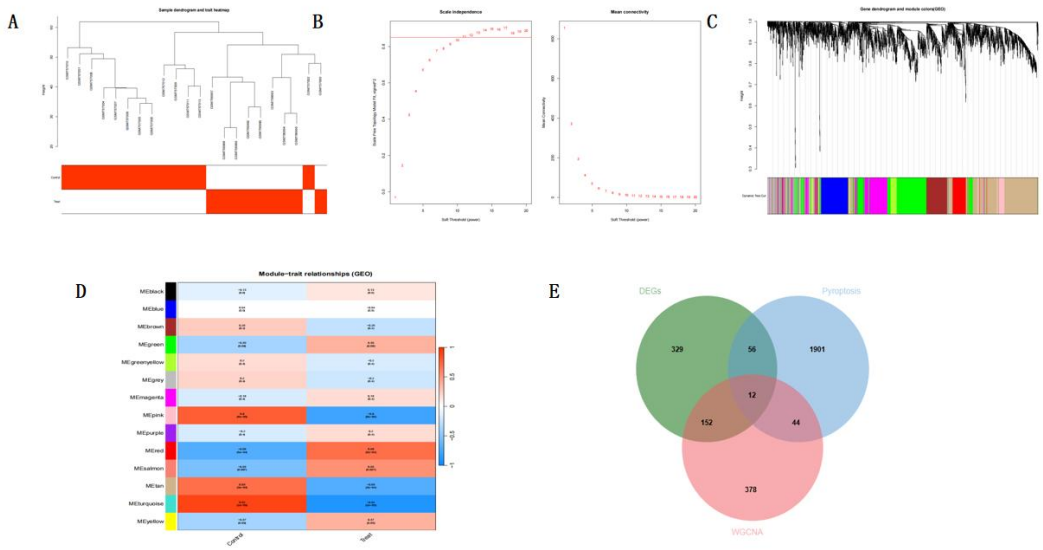


Figure 3 WGCNA of pyro DEGs

2.4 Identification of Hub Genes

Among the 12 overlapping genes, Lasso regression algorithm screened 7 genes (Figure 4A), RF algorithm and SVM-RFE analysis selected 4 genes (Figure 4B and C) respectively, and then, the intersection of the three was taken to obtain two hub genes, namely *MYH9* and *CDC20* (Figure 4D).

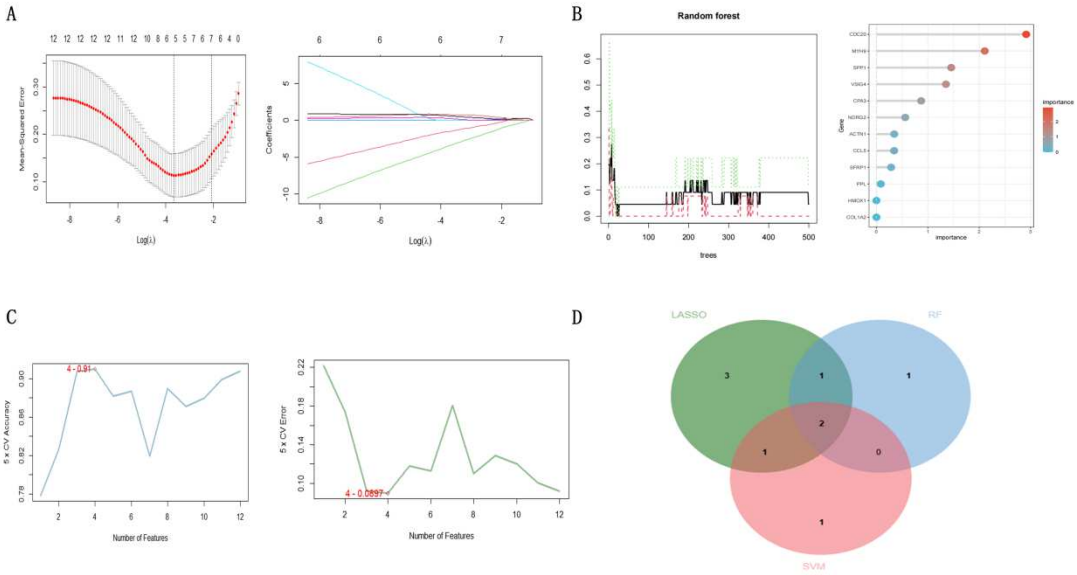


Figure 4 Machine learning screening hub genes

2.5 Expression of Hub Genes and ROC Validation

We performed analysis of the hub genes and found that *CDC20* exhibited higher expression in DN across both datasets, while *MYH9* exhibited relatively lower expression in DN (Figure 5A and 5B). Furthermore, ROC analysis of the two datasets demonstrated that both hub genes possessed good diagnostic performance for DN, with AUC values exceeding 0.68. In the GSE30528 dataset, *MYH9* exhibited an AUC of 0.923 and *CDC20* an AUC of 0.991; in the GSE96804 dataset, *MYH9* exhibited an AUC of 0.683 and *CDC20* exhibited an AUC of 0.832 (Figure 5C and 5D).

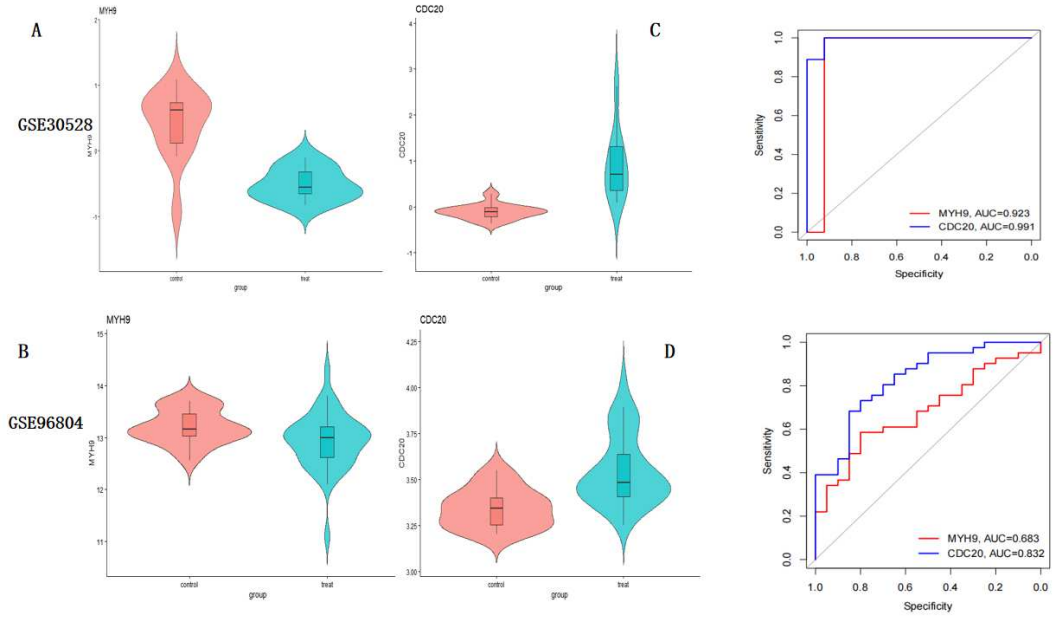


Figure 5 Expression of hub gene and ROC verification

2.6 GSEA Analysis

We first calculated Spearman's correlation analysis among *MYH9*, *CDC20*, and all detected genes to obtain a list of correlated genes. Subsequently, we sorted enriched pathways by *p*-value and selected the top five pathways with the lowest *p*-values to plot enrichment curves. Results showed that *MYH9* was highly enriched in nephron development, actin filament organization, and cytoskeletal organization (Figure 6A and 6B), suggesting *MYH9* may participate in glomerular morphogenesis by regulating actin dynamics. *CDC20* showed high enrichment in mitochondrial matrix, ribosomal subunits, and abnormal morphology of lymphocytes and T cells (Figure 6C and 6D), suggesting that *CDC20* may contribute to DN progression through cellular homeostasis and inflammatory responses.

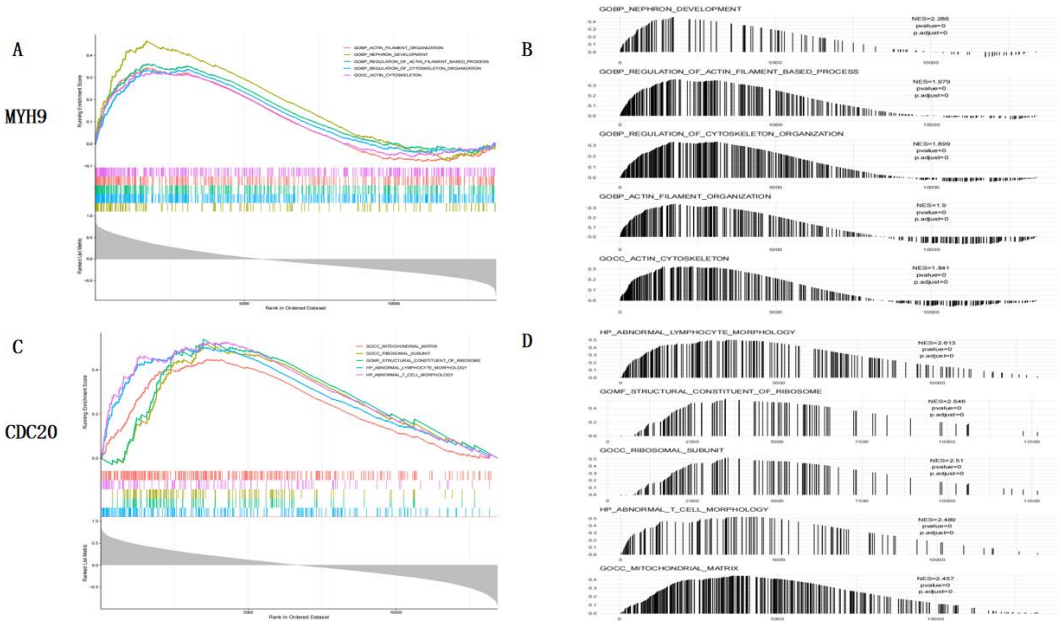


Figure 6 GSEA analysis of hub genes

2.7 Immune Cell Infiltration Analysis

An overview of the relative abundance across 22 immune cell types for each sample is provided in Figures 7A and 7B. Positive correlations were detected between resting dendritic cells and activated dendritic cells (r=0.69), CD4 naive T cells and γδ T cells (r=0.63), memory B cells and CD4 naive T cells (r=0.63), among others (Figure 7C). DN differed significantly from the normal group in three immune cell types (p<0.05): T cells. γδ T cells, resting mast cells, and M2 macrophages were more abundant in DN (Figure 7D). Additionally, Pearson's correlation analysis of the hub genes *MYH9* and *CDC20* revealed positive correlations: *MYH9* correlated with resting mast cells (r=0.5) (Figure 7E); while *CDC20* showed positive correlations with M2 macrophages (r=0.58), resting mast cells (r=0.71), CD4 naive T cells (r=0.64), and γδ T cells (r=0.57) (Figure 7F).

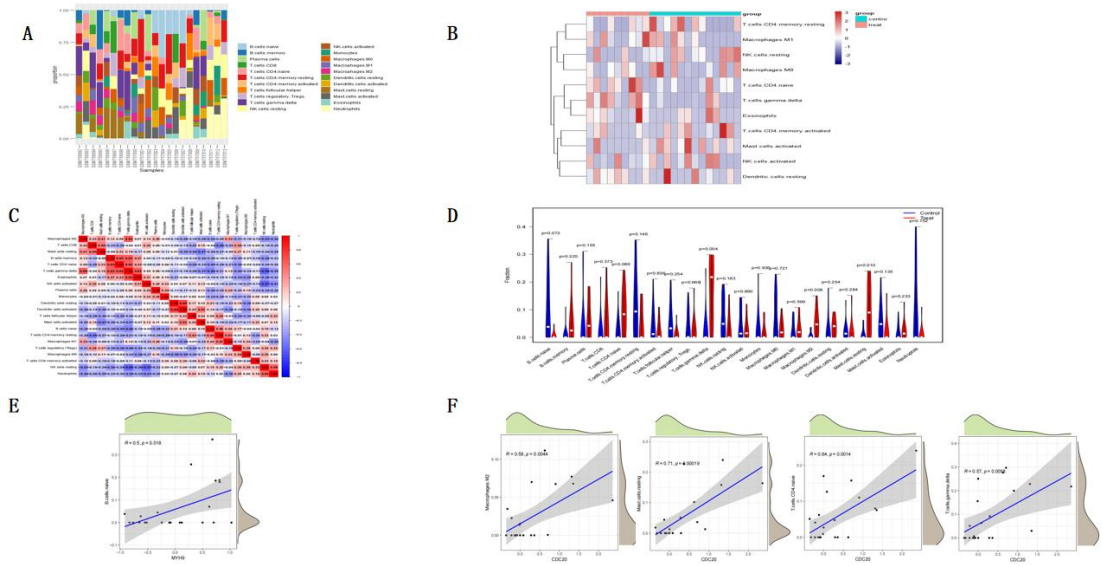


Figure 7 Immune infiltration analysis

2.8 Monocyte RNA Sequencing

Sequencing identified the distribution of *MYH9* and *CDC20* across 12 cell clusters (Figure 8A), with both genes highly expressed in podocytes (Figures 8B and C).

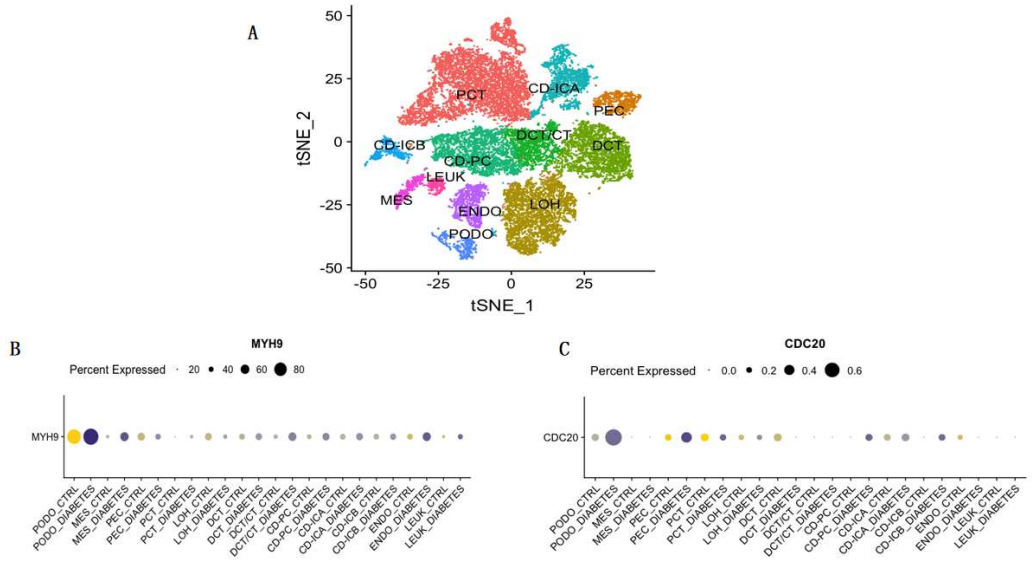


Figure 8 Results of mononuclear RNA sequencing

2.9 Drug Prediction and Molecular Docking

We used the dsigdb database in enrichr platform to predict the potential drugs for *MYH9* and *CDC20*. The results showed that genistein, calpain inhibitor I, deferoxamine and other drugs may have therapeutic potential for DN. Then, according to the *p* value of binding drugs and their ability to enrich hub genes, we finally selected genistein as a potential drug for molecular docking. Molecular docking results illustrated that genistein had strong binding activity to both hub genes, and the binding energy of genistein to *MYH9* was -7.2 kcal/mol; The binding energy of *CDC20* was -8.2 kcal/mol, indicating that genistein may have a potential molecular mechanism for targeted therapy of DN(Figure 9A and B).

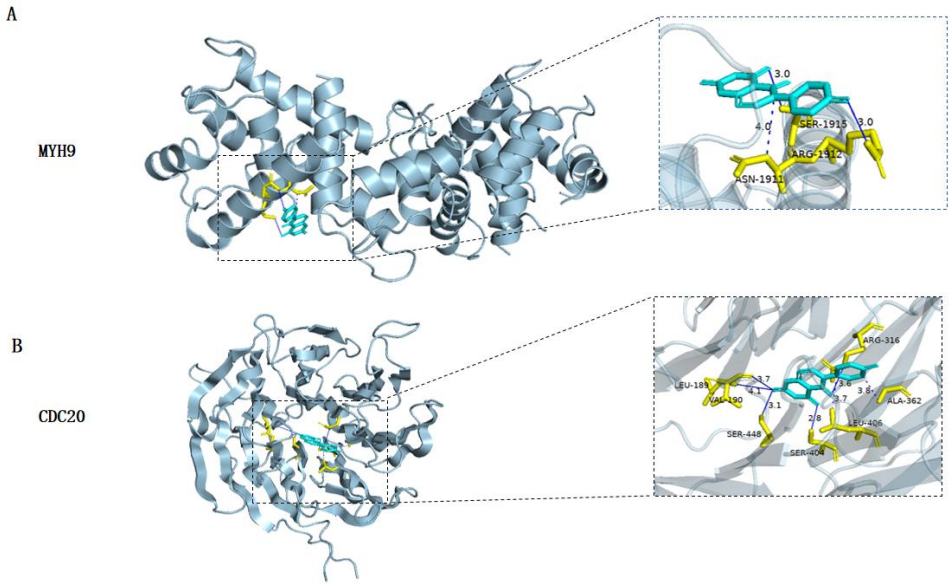


Figure 9 Schematic diagram of drug prediction and molecular docking results of hub genes

2.10 Construction of the Core ceRNA Network

Using miRNet, miRDB and Starbase databases, we predicted miRNAs associated with *MYH9* and *CDC20*, and obtained 40 pairs of mRNA-miRNA interactions. Subsequently, we used the Starbase database to predict the lncRNA corresponding to miRNA, and obtained 156 pairs of miRNA-lncRNA interactions.

Finally, Cytoscape 3.9.1 software was employed to generate the ceRNA regulatory network, which contained 65 nodes (28 miRNAs, 2 mRNAs and 35 lncRNA) and 157 edges (Figure 10).

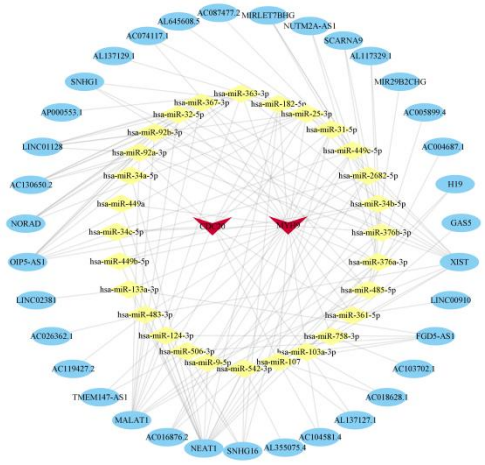


Figure 9Construction of ceRNA network

Discussion

The annual incidence of DN in China continues to rise, and the affected population is becoming younger. Its pathological mechanism is complex, involving podocyte injury, hemodynamic changes, inflammatory reaction and other links. At present, the treatment of DN is limited, and there is no specific diagnosis and treatment measures. Therefore, new molecular approaches are urgently needed to help the early diagnosis and treatment of DN. Pyroptosis, as a new way of death to release inflammatory factors and expand inflammatory response, has gradually appeared in the field of vision of researchers. With the in-depth study of pyroptosis, its key role in the progress of DN has been gradually confirmed. However, the molecular mechanism of pyroptosis promoting DN is still unclear, and the mechanism of pyroptosis in DN needs further study. In this context, we analyzed the common molecular mechanism of pyroptosis and DN. First, we analyzed the difference between DN and normal samples, and obtained 549 DEGs. Then, we took the intersection with the pyroptosis expression genes for go and KEGG analysis. Then, we screened the intersection genes by WGCNA and machine learning, and obtained *MYH9* and *CDC20* genes. We analyzed the expression of these two genes and verified

the ROC curve, which confirmed their strong predictability and stability.

Immunity is important in the development of DN[32,33]. Our findings show that γδ T cells, resting mast cells, and M2 macrophages have higher levels in DN samples, suggesting they may be involved in DN through pyroptosis. γδ T cells, a key part of T cells, cause kidney fibrosis by releasing cytokines like interleukin-2. This leads to epithelial-to-mesenchymal transition (EMT) in the kidney and speeds up kidney disease in mice[34]. M2 macrophages, a common immune cell in DN, gather to cause kidney fibrosis and worsen kidney function. Macrophages are divided into M1 and M2 types. M1 macrophages are more common in the early stages of kidney injury and cause inflammation. If the injury is not controlled early, it leads to more M2 macrophages, which turn into myofibroblasts and promote fibrosis[35]. This fibrosis causes kidney tissue to shrink and replace normal kidney tissue, leading to low oxygen and poor blood flow, which speeds up DN. Resting mast cells are also linked to kidney function in DN. Mast cells are mostly in the kidney tubulointerstitial space and are connected to chronic inflammation and kidney fibrosis. They also act as markers of tissue damage, releasing substances like histamine and heparin that activate myofibroblasts and increase collagen, speeding up DN[36]. Overall, these findings show that γδ T cells, resting mast cells, and M2 macrophages exert a pro-inflammatory role in DN, consistent with our results. Finally, Pearson correlation analysis of the pivotal genes *MYH9* and *CDC20* revealed positive correlations with resting mast cells, M2 macrophages, naive CD4 T cells, and γδ T cells. These findings indicate that both genes play crucial roles in promoting pyroptosis and shaping the DN immune microenvironment.

Studies show that *MYH9* and *CDC20* are mainly found in podocytes in the kidney[37,38], which matches our single-nuclear RNA sequencing results. *MYH9* mutations are usually linked to blood disorders like congenital macrothrombocytopenia. However, E Jing et al[39]. found a patient with an *MYH9* mutation who did not have blood problems but had DN. Abnormal *MYH9* expression affects the cytoskeleton, causing protein in the urine and kidney failure. And high *MYH9* levels in DN patients also cause EMT in kidney tissue, leading to fibrosis and

speeding up DN. This matches our GSEA results, which show that *MYH9* is involved in kidney development and cytoskeletal regulation. Another study found that removing *MYH9* reduces α-SMA and type I collagen, which helps reduce kidney fibrosis in mice[40]. Meanwhile, the more severe the DN fibrosis, the worse the kidney function, reducing fibrosis can reduce inflammation through nuclear factor kappa-B (NF-κB) and protect kidney function. Additionally, *CDC20* also has important effects in the kidney. High *CDC20* activity raises serum creatinine and protein in urine in mice, while blocking *CDC20* can improve kidney function and reduce damage[41,42]. Other research shows that *CDC20* increases caspase-3, which controls pyroptosis, apoptosis, autophagy, and cell division, which matches our GSEA results[43]. The above evidence collectively demonstrates that *MYH9* and *CDC20* play crucial roles in the early prediction and progression of DN. Predicting the expression of these two pivotal genes could aid in the early intervention and treatment of DN.

We did drug prediction for two key genes and found that genistein could be a potential treatment. Genistein, the most active compound in soy isoflavones, can stop reactive oxygen species (ROS) production and GSDMD-mediated cell damage, which prevents the release of inflammatory substances[44]. Li et al.[45] found that genistein lowers blood glucose and serum creatinine levels in DN rats. It also reduces inflammation and stops mesangial matrix expansion, helping improve kidney damage. Further studies showed that genistein has strong antioxidant properties. On the one hand, it blocks NF-κB activation, which reduces ROS production. On the other hand, genistein also improves mitochondrial membrane potential, helps make mitochondrial fusion protein 2, and keeps mitochondrial DNA stable, which slows DN progression. Additionally, genistein reduces leukocyte adhesion and stops inflammatory cells from releasing in the kidneys, lowering pro-fibrotic factors[46]. In summary, these properties of demethylated lignan enable it to effectively inhibit the progression of DN. In our study, molecular docking of genistein with *MYH9* and *CDC20* showed strong binding: -7.2 kcal/mol with *MYH9* and -8.2 kcal/mol with *CDC20*, suggesting that genistein could effectively stop DN.

We built a ceRNA network to find potential regulatory targets and pathways for

DN. While ceRNA networks are often studied in neurological and cancer diseases, they have not been widely used in DN research. This study created a ceRNA network with *MYH9* and *CDC20*, which includes 28 miRNAs, 2 mRNAs, and 35 lncRNAs, to explore ceRNA roles in DN. Among these, the lncRNA NEAT1 plays a key role in promoting DN through pyroptosis. Studies show that blocking NEAT1 reduces caspase-1 and GSDMD-N expression in DN rats, improving fibrosis and kidney damage. It was also found that NEAT1 promotes DN by regulating miR-34c. MiR-34c. As a negative regulatory factor upstream of NLRP3, miR-34c can reduce the expression of NLRP3 and caspase-1 and other pyroptosis-related factors in DN, thereby alleviating the inflammatory response, reducing oxidative stress and the occurrence of fibrosis[47]. Another study showed that blocking *CDC20* reduces caspase-3, decreases inflammation, and improves kidney function[43]. These findings suggest that the NEAT1/miR-34c-5p/*CDC20* pathway helps activate pyroptosis, which drives DN progression.

MALAT1 has been proved to be related to inflammation and cell death in a variety of diseases. By establishing a mouse model of acute kidney injury, it was found that MALAT1 knockdown can significantly reduce the expression of GSDMD, caspase-1, NLRP3 and other pyroptosis markers, as well as IL-1 β, IL-18 and other inflammatory cytokines, thereby effectively reducing renal inflammation and cell death[48]. Meanwhile, in a HG-induced DN mouse model, MALAT1 levels were higher along with increased oxidative stress and pyroptosis[49]. These studies show that MALAT1 is involved in kidney disease progression by controlling pyroptosis. Targeting MALAT1 may provide new treatments and diagnostic approaches for DN. lncRNA XIST is highly expressed in DN patients. In streptozotocin induced DN rat model and HG induced HK-2, silencing XIST can inhibit NLRP3 mediated apoptosis of renal tubular epithelial cells, thereby reducing DN induced renal metabolic abnormalities and renal injury[50]. In addition, as a new type of lncRNA, FGD5-AS1 expression is significantly increased in ESRD, which can produce pro-inflammatory factors, damage glomerular filtration function, increase serum creatinine, urea nitrogen, blood pressure, serum albumin and other biochemical indicators, and then

aggravate renal injury. FGD5-AS1 can also disorder lipid metabolism, and lipid disorder is the determining factor leading to DN, which further confirms the importance of FGD5-AS1 in DN[51]. Reports show that lncRNA OIP5-AS1 is involved in the progression of DN. Increased levels of OIP5-AS1 have been found in DN mice and hyperglycemia-induced HK-2 cells. This higher expression promotes EMT and kidney fibrosis in hyperglycemia-treated HK-2 cells[52]. Another study found that there was a decrease in miR-25-3p expression in the DN group. When the level of OIP5-AS1 was knocked down, the expression of miR-25-3p increased, accompanied by an increase in cell viability, as well as a reduction in cell apoptosis and oxidative stress levels[53]. These results suggest that OIP5-AS1 may affect oxidative stress and fibrosis in DN by controlling miR-25-3p levels. In this study, miR-25-3p regulates DN through *MYH9*, a direct target. The two genes are negatively linked: miR-25-3p lowers *MYH9* levels, which reduces EMT and slows fibrosis and DN[54,40]. Thus, We believe that the NEAT1/miR-34c-5p/*CDC20* and OIP5-AS1/miR-25-3p/*MYH9* pathways may be key regulators in the early stages and diagnosis of DN.

In conclusion, this work comprehensively analyzed the molecular mechanism of pyroptosis in DN. Two DN related oncogenes (*MYH9* and *CDC20*) were screened by WGCNA and machine learning. The stability and predictability of the two genes were confirmed by expression analysis and ROC verification, which provided a new basis for the development mechanism of DN at the transcriptome level. In addition, through GSEA analysis of hub genes, the correlation between hub genes and immune cells was analyzed, and the molecular mechanism of the two hub genes was explored by constructing ceRNA network and molecular docking. However, this study has some limitations. First, the sample size for analysis is relatively small; Second, there is a lack of further in vivo and in vitro experimental verification. Therefore, we should explore this conclusion more deeply in the future, so as to provide new ideas for the early intervention and diagnosis of DN.

Data availability

The datasets (GSE30528) analyzed in this study were derived from the Gene Expression Omni-bus (GEO) database (https://www.ncbi.nlm.nih.gov/geo/).

Author Contribution Statement

Xinru Wang and Zhaoan Guo jointly conceived the research and wrote the main text of the manuscript. Xinru Wang conducted data mining, bioinformatics analysis, and prepared charts, while Zhaoan Guo reviewed the article and provided funding support. All authors declare that there is no conflict of interest.

Funding Declaration

Supported by Shandong Natural Science Foundation Project (No. ZR2022LZY005)

References

[1] 中华中医药学会,北京中医药大学东直门医院,北京中医药大学.糖尿病肾脏疾病中西医结合诊疗指南[J].北京中医药大学学报,2024,47(04):580-592.
[2] Chen J, Liu D, Lei L, et al. CNPY2 Aggravates Renal Tubular Cell Ferroptosis in Diabetic Nephropathy by Regulating PERK/ATF4/CHAC1 Pathway and MAM Integrity. Adv Sci (Weinh). 2025 Jul;12(25):e2416441.
[3] Jin Q, Liu T, Qiao Y, et al. Oxidative stress and inflammation in diabetic nephropathy: role of polyphenols. Front Immunol. 2023 Jul 21;14:1185317.
[4] Li J, Wang X, Jia W, et al. Association of the systemic immuno-inflammation index, neutrophil-to-lymphocyte ratio, and platelet-to-lymphocyte ratio with diabetic microvascular complications. Front Endocrinol (Lausanne). 2024 Apr 10;15:1367376.
[5] Tsai IN, Tsai YC, Huang HP, et al. Protective Effect of Neochlorogenic Acid on Diabetic Nephropathy via Inflammation and Pyroptosis Suppression. J Agric Food Chem. 2025 Oct 22;73(42):26763-26779.
[6] Wang L, Xie X, Chen Q, et al. Puerarin reduces diabetic nephropathy-induced podocyte pyroptosis by modulating the SIRT1/NLRP3/caspase-1 pathway. Mol Cell Endocrinol. 2025 Jan 1;595:112409.
[7] Zhou Z, Li Q. The Role of Pyroptosis in the Pathogenesis of Kidney Diseases. Kidney Dis (Basel). 2023 Jun 24;9(6):443-458.
[8] Zhang Z, Hu H, Luo Q, et al. Dihydroxyacetone phosphate accumulation leads to podocyte pyroptosis in diabetic kidney disease. J Cell Mol Med. 2024 Feb;28(3):e18073.
[9] Lan J, Xu B, Shi X, et al. WTAP-mediated N6-methyladenosine modification of NLRP3 mRNA in kidney injury of diabetic nephropathy. Cell Mol Biol Lett. 2022 Jun 27;27(1):51.
[10] Wen S, Deng F, Li L, et al. VX-765 ameliorates renal injury and fibrosis in diabetes by regulating caspase-1-mediated pyroptosis and inflammation. J Diabetes Investig. 2022 Jan;13(1):22-33.
[11] Yuan S, Wang Y, Li Z, et al. Gasdermin D is involved in switching from apoptosis to pyroptosis in TLR4-mediated renal tubular epithelial cells injury in diabetic kidney disease. Arch Biochem Biophys. 2022 Sep 30;727:109347.
[12] Li L, Zhang L, Cai Y, et al. DNA damage-induced AIM2 pyroptosis in high glucose-induced proximal tubular epithelial cell. Front Cell Dev Biol. 2024 Nov 26;12:1457369.
[13] Zhang M, Xue SJ, Yang F, et al. LncRNA SNHG7/miR-181b-5p/TLR4 Activates Inflammation And Promotes Pyroptosis Through NF-κB Signaling in Diabetic Nephropathy. Inflammation. 2025

Dec;48(6):3828-3840.
[14] Sunilkumar S, Subrahmanian SM, Yerlikaya EI, et al. REDD1 expression in podocytes facilitates renal inflammation and pyroptosis in streptozotocin-induced diabetic nephropathy. Cell Death Dis. 2025 Feb 7;16(1):79.
[15] Shahzad K, Fatima S, Khawaja H, et al. Podocyte-specific Nlrp3 inflammasome activation promotes diabetic kidney disease. Kidney Int. 2022 Oct;102(4):766-779.
[16] Wu M, Han W, Song S,et al. NLRP3 deficiency ameliorates renal inflammation and fibrosis in diabetic mice. Mol Cell Endocrinol. 2018 Dec 15;478:115-125.
[17] Yang P, Fan L, Yuan D, et al, Huang Y. CUEDC2 improves pyroptosis and kidney damage in diabetic kidney disease by inhibiting NLRP3 inflammasome activation. Cell Signal. 2026 Feb;138:112239.
[18] Li S, Wang J, Chen Y, et al. Canagliflozin Attenuates Podocyte Inflammatory Injury through Suppressing the TXNIP/NLRP3 Signaling Pathway in Diabetic Kidney Disease Mice. Inflammation. 2025 Oct;48(5):3180-3193.
[19] Ritchie ME, Phipson B, Wu D,et al. limma powers differential expression analyses for RNA-sequencing and microarray studies. Nucleic Acids Res. 2015 Apr 20;43(7):e47.
[20] Kanehisa M, Furumichi M, Sato Y, et al. KEGG: biological systems database as a model of the real world. Nucleic Acids Res. 2025 Jan 6;53(D1):D672-D677.
[21] The Gene Ontology Consortium. The Gene Ontology Resource: 20 years and still GOing strong. Nucleic Acids Res. 2019 Jan 8;47(D1):D330-D338.
[22] Langfelder P, Horvath S. WGCNA: an R package for weighted correlation network analysis. BMC Bioinformatics. 2008 Dec 29;9:559.
[23] Kaneko S, Hirakawa A, Hamada C. Enhancing the Lasso Approach for Developing a Survival Prediction Model Based on Gene Expression Data. Comput Math Methods Med. 2015;2015:259474.
[24] Xiong Y, Ling QH, Han F, et al. An efficient gene selection method for microarray data based on LASSO and BPSO. BMC Bioinformatics. 2019 Dec 30;20(Suppl 22):715.
[25] Izmirlian G. Application of the random forest classification algorithm to a SELDI-TOF proteomics study in the setting of a cancer prevention trial. Ann N Y Acad Sci. 2004 May;1020:154-74. doi: 10.1196/annals.1310.015. PMID: 15208191.
[26] Sanz H, Valim C, Vegas E, et al. SVM-RFE: selection and visualization of the most relevant features through non-linear kernels. BMC Bioinformatics. 2018 Nov 19;19(1):432.
[27] Robin X, Turck N, Hainard A, et al. pROC: an open-source package for R and S+ to analyze and compare ROC curves. BMC Bioinformatics. 2011 Mar 17;12:77.
[28] Yu G, Wang LG, Han Y, et al. clusterProfiler: an R package for comparing biological themes among gene clusters. OMICS. 2012 May;16(5):284-7.
[29] Subramanian A, Tamayo P, Mootha VK,et al. Gene set enrichment analysis: a knowledge-based approach for interpreting genome-wide expression profiles. Proc Natl Acad Sci U S A. 2005 Oct 25;102(43):15545-50.
[30] Newman AM, Steen CB, Liu CL, et al. Determining cell type abundance and expression from bulk tissues with digital cytometry. Nat Biotechnol. 2019 Jul;37(7):773-782.
[31] Wilson PC, Wu H, Kirita Y, Uchimura K, Ledru N, Rennke HG, et al. The single-cell transcriptomic landscape of early human diabetic nephropathy. Proc Natl Acad Sci United States America (2019) 116:19619 – 25.
[32] Wang Y, Liu Y, Gu W, et al. Association of immune-inflammation indexes with incidence and prognosis of diabetic nephropathy: a systematic review and meta-analysis. Front Endocrinol (Lausanne). 2025 Aug 18;16:1532682.
[33] Zhou W, Zeng Z, Li X, et al. Comprehensive Analysis and Experimental Validation of Immune-Related Biomarkers and Immune Microenvironment in Diabetic Nephropathy. J Inflamm Res. 2025 Oct 3;18:13711-13726.
[34] Sun H, Wang X, Liu Y,et al. Thymocytes induce renal tubular epithelial cells to undergo the epithelial-to-mesenchymal transition. Asian Pac J Allergy Immunol. 2025 Mar;43(1):111-123.
[35] Deng L, Ouyang B, Tang W, et al. Icariside II modulates pulmonary fibrosis via PI3K/Akt/ β -catenin pathway inhibition of M2 macrophage program. Phytomedicine. 2024 Jul 25;130:155687.
[36] Varol H, van der Elst G, Baan CC,et al. Mast Cells in Kidney Transplant Biopsies With

Borderline T Cell-mediated Rejection and Their Relation to Chronicity. Transplant Direct. 2023 Apr 20;9(5):e1480.
[37] Otterpohl KL, Busselman BW, Zimmerman JL,et al. Thick Ascending Limb Specific Inactivation of Myh9 and Myh10 Myosin Motors Results in Progressive Kidney Disease and Drives Sex-specific Cellular Adaptation in the Distal Nephron and Collecting Duct. Function (Oxf). 2025 Feb 12;6(1):zqae048.
[38] Wu F, Sun Y, Chen J, et al. The Oncogenic Role of APC/C Activator Protein Cdc20 by an Integrated Pan-Cancer Analysis in Human Tumors. Front Oncol. 2021 Aug 30;11:721797.
[39] 鄂静,马丹娜,刘顺瑶,等.MYH9 基因突变伴糖尿病肾脏疾病一例报道[J].中国糖尿病杂志,2023,31(05):382-385.
[40] Wang F, Suo XG, Wang JN, et al. SFN promotes renal fibrosis via binding with MYH9 in chronic kidney disease. Eur J Pharmacol. 2024 Sep 15;979:176806.
[41] Swanson M, Yun J, Collier DM,et al. Identification of cell division cycle protein 20 in various forms of acute and chronic kidney injury in mice. Am J Physiol Renal Physiol. 2023 Aug 1;325(2):F248-F261.
[42] He J, Xu S, Jiang M, et al. CDC20 inhibition alleviates fibrotic response of renal tubular epithelial cells and fibroblasts by regulating nuclear translocation of β-catenin. Biochim Biophys Acta Mol Basis Dis. 2023 Apr;1869(4):166663
[43] You R, Li Y, Jiang Y, et al. WWP2 deletion aggravates acute kidney injury by targeting CDC20/autophagy axis. J Adv Res. 2025 May;71:471-485.
[44] Yang M, Zhang T. Genistein inhibits the release of pro-inflammatory substances from macrophages by suppressing potassium loss- and ROS-mediated caspase-1/gasdermin D pathway activation and pyroptotic cell lysis. Iran J Basic Med Sci. 2024;27(12):1506-1514.
[45] Li Y, Ou S, Liu Q,et al. Genistein improves mitochondrial function and inflammatory in rats with diabetic nephropathy via inhibiting MAPK/NF-κB pathway. Acta Cir Bras. 2022 Aug 15;37(6):e370601.
[46] Al-Bazi MM, Banjabi AA, Khalifa FK,et al. The exploration of therapeutic potential of bioflavonoids in metabolic acidosis and inflammation-associated with acute kidney injury: Therapeutic potential of bioflavonoids in acute kidney injury. Int J Health Sci (Qassim). 2025 Mar-Apr;19(2):57-65.
[47] Zhan JF, Huang HW, Huang C, et al. Long Non-Coding RNA NEAT1 Regulates Pyroptosis in Diabetic Nephropathy via Mediating the miR-34c/NLRP3 Axis. Kidney Blood Press Res. 2020;45(4):589-602.
[48] Guo P, Deng G, Li L, et al. MALAT1's m6A Modification by METTL3 Promotes Pyroptosis and Inflammation in Sepsis-Induced Acute Kidney Injury in Mice. J Inflamm Res. 2025 Oct 24;18:14663-14678.
[49] Zuo Y, Chen L, He X,et al. Atorvastatin Regulates MALAT1/miR-200c/NRF2 Activity to Protect Against Podocyte Pyroptosis Induced by High Glucose. Diabetes Metab Syndr Obes. 2021 Apr 13;14:1631-1645.
[50] Xu J, Wang Q, Song YF, et al. Long noncoding RNA X-inactive specific transcript regulates NLR family pyrin domain containing 3/caspase-1-mediated pyroptosis in diabetic nephropathy. World J Diabetes. 2022 Apr 15;13(4):358-375.
[51] Ajorlou P, Hosseini SA, Ghanbarnejad A, et al. FGD5-AS1 and Th1/Th2 imbalance in the progression of diabetic nephropathy: evidence from bioinformatic and experimental validation. Clin Exp Med. 2025 Nov 25;26(1):38.
[52] Fu JX, Sun GQ, Wang HL,et al. LncRNA OIP5-AS1 induces epithelial-to-mesenchymal transition and renal fibrosis in diabetic nephropathy via binding to miR-30c-5p. J Biol Regul Homeost Agents. 2020 May-Jun;34(3):961-968.
[53] 杨娟,张厚芬,吴松,等.LncRNA OIP5-AS1 调节 miR-25-3p/SOX4 轴对高糖诱导的人肾小管上皮细胞生物学过程的影响[J].天津医药,2023,51(02):131-138.
[54] Niu M, Feng Y, Zhang N,et al. High expression of miR-25 predicts favorable chemotherapy outcome in patients with acute myeloid leukemia. Cancer Cell Int. 2019 May 7;19:122.